Research Square

Preprints are preliminary reports that have not undergone peer review.
They should not be considered conclusive, used to inform clinical practice,
or referenced by the media as validated information.

Green synthesis and characterization of Mesosphaerum suaveolens-loaded chitosan nanoparticles: An in vitro evaluation

Lakshmanan Subramani
Annamalai University
Arthi Karunakaran
Annamalai University
Vijayakumar Natesan
Annamalai University
Sankar Madhavan
Rajalakshmi Engineering College
Sheeladevi Samynathan
Bharathidasan College of Arts and Science (Autonomous)
Sekar Vijayakumar
Thiagarajar College
Ganapathy Sindhu
Annamalai University
Lakshmanan Vennila
vennilajnr@gmail.com

Annamalai University

Research Article

Keywords: Mesosphaerum suaveolens, Chitosan nanoparticles, green synthesis, Antioxidant activity, Anticancer activity

Posted Date: September 24th, 2026

DOI: https://doi.org/10.21203/rs.3.rs-10918137/v1

License: This work is licensed under a Creative Commons Attribution 4.0 International License.
Read Full License

Additional Declarations: No competing interests reported.

Green synthesis and characterization of *Mesosphaerum suaveolens*-loaded chitosan nanoparticles: An *in vitro* evaluation

Lakshmanan Subramani[1], Arthi Karunakaran[1], Vijayakumar Natesan[1], Sankar Madhavan [2], Sheeladevi Samynathan[3], Sekar Vijayakumar[4,5], Ganapathy Sindhu[1], Lakshmanan Vennila[1]*

[1]*Department of Biochemistry & Biotechnology, Faculty of sciences, Annamalai University, Chidambaram-608 002, India.*

[2]*Department of Biotechnology, Faculty of sciences, Rajalakshmi Engineering College, Chennai-602105, India.*

[3]*Department of Biochemistry, Bharathidasan College of Arts and Science (Autonomous), Erode-638116, India.*

[4]*Department of Zoology, Thiagarajar College, (Affiliated to Madurai Kamaraj University), Madurai-625 009, India.*

[5]*The National Centre of Excellence on Statistical and Mathematical Modelling on Bioresource Management, Thiagarajar College, (Affiliated to Madurai Kamaraj University), Madurai-625 009, India*

*Corresponding author:

Email Address: vennilajnr@gmail.com (Dr. LakshmanaVennila)

Abstract

Mesosphaerum suaveolens is a medicinal plant rich in bioactive phytochemicals with diverse biological properties. Green synthesis using plant-derived compounds provides an eco-friendly approach for developing biologically active nanoparticles. Chitosan is a biocompatible and biodegradable polymer widely used in nanoparticle preparation. The present study aimed to synthesize chitosan nanoparticles using *M. suaveolens* leaf extract and evaluate their biological activities. The ionic gelation technique was employed for the synthesis of chitosan nanoparticles. UV–Visible spectroscopy, FTIR, XRD, and SEM–EDX were employed to characterize the synthesized nanoparticles. Antioxidant activity was evaluated using DPPH and ABTS assays. MsCNPs showed a characteristic absorption peak at 225 nm and functional groups associated with nanoparticle formation. The nanoparticles exhibited antioxidant activity with IC_{50} values of 20 µg/mL for DPPH and 15 µg/mL for ABTS. Concentration-dependent antibacterial activity was observed against the tested bacterial strains. MsCNPs also showed anticancer activity against MCF-7 cells, with an IC_{50} of approximately 40 µg/mL and increased apoptotic changes. Overall, the findings demonstrate that *M. suaveolens* mediated chitosan nanoparticles possess promising antibacterial, antioxidant and anticancer properties, highlighting their potential for biomedical and pharmaceutical applications.

Keywords: *Mesosphaerum suaveolens*, Chitosan nanoparticles, green synthesis, Antioxidant activity, Anticancer activity.

Introduction

Nanotechnology is a rapidly developing interdisciplinary field focused on the development and utilization of materials at the nanometer scale. At this dimension, materials exhibit distinctive physicochemical characteristics, including a greater surface-area-to-volume ratio, increased reactivity, and enhanced interactions with biological systems. These properties have expanded the applications of nanomaterials in medicine, drug delivery, diagnostics, antimicrobial therapy, and cancer treatment [1,2]. Among various polymeric nanoparticles, nanomaterials have attracted considerable interest as efficient carriers for bioactive compounds because of their ability to improve solubility, stability, cellular uptake, targeted delivery, and controlled release.

Chitosan, a naturally derived biodegradable and biocompatible polymer, is particularly suitable for nanoparticle development because of its cationic nature, mucoadhesive properties, low toxicity, and ease of functionalization. Chitosan nanoparticles have demonstrated promising antioxidant, antimicrobial, and anticancer properties and can facilitate the delivery of therapeutic compounds to target cells. Their biological activity can be further enhanced through the incorporation of plant-derived bioactive compounds.

Green synthesis provides a sustainable alternative to conventional nanoparticle production by utilizing biological resources such as plant extracts. Plant phytochemicals, including phenolics, flavonoids, terpenoids, alkaloids, and other secondary metabolites, can contribute to nanoparticle formation and stabilization while also imparting additional biological activity. This approach offers advantages such as reduced use of hazardous chemicals, lower energy requirements, cost-effectiveness, and improved biological compatibility [3,4].

M. suaveolens, a medicinal plant belonging to the family *Lamiaceae*, is traditionally used for various ailments and is reported to possess antioxidant, antimicrobial, anti-inflammatory, and other pharmacological properties. Its diverse phytochemical constituents make it a promising candidate for incorporation into nanoparticle-based systems. The combination of *M. suaveolens*bioactive compounds with chitosan nanoparticles may therefore provide a multifunctional platform with enhanced biological properties.

Oxidative stress and microbial infections are major contributors to several pathological conditions, while uncontrolled cellular proliferation remains a significant challenge in cancer

management. Plant-derived chitosan nanoparticles may address these challenges through free-radical scavenging, antimicrobial action, modulation of cellular pathways, and induction of cancer cell death. In particular, their potential to enhance intracellular delivery and promote apoptosis provides a promising approach for anticancer applications.

The present study focuses on the green synthesis and characterization of *M. suaveolens* chitosan nanoparticles (MsCNPs) and their *in vitro* antioxidant, antimicrobial, and anticancer activities. The study aims to explore the physicochemical characteristics of the synthesized nanoparticles and evaluate their potential biological activities, thereby highlighting their prospective application as sustainable nanomaterials for biomedical research.

Materials and method

Plant authentication and extract preparation

The leaves of *M. suaveolens* (L.) Kuntze were collected and authenticated based on their characteristic morphological features. The plant was identified according to its taxonomic and botanical characteristics and confirmed as belonging to the family *Lamiaceae*. The systematic position of the plant was recorded as follows:

Kingdom	:	Plantae
Division	:	Angiosperms
Class	:	Eudicots
Order	:	Lamiales
Family	:	*Lamiaceae*
Genus	:	*Mesosphaerum*
Species	:	*suaveolens*

The identification was supported by characteristic features of the species, including an aromatic herbaceous habit, quadrangular hairy stems, opposite and simple leaves, dense glandular hairs, and globose clusters of bluish-purple to lavender flowers. These morphological characteristics were used for the authentication of the plant material prior to extract preparation.

Synthesis of MsCNPs

Chitosan nanoparticles were synthesised using *M. suaveolens* leaf extract by the ionic gelation method. Fresh leaves were collected, washed thoroughly, dried, and powdered. The leaf extract was obtained by heating the powdered leaves in distilled water and subsequently filtering the mixture to remove particulate matter and collect a clear filtrate. A chitosan solution (0.5–1% w/v) was prepared by dissolving chitosan in 1% acetic acid with constant stirring. The resulting solution was then adjusted to a pH range of approximately 4.5–5.5. A freshly prepared sodium tripolyphosphate (TPP) solution (0.1–0.5% w/v) was used as a crosslinking agent. The leaf extract was added dropwise to the chitosan solution under constant stirring, followed by the slow addition of TPP solution. The addition of TPP to the chitosan solution promoted ionic cross-linking, leading to nanoparticle formation through attraction between the oppositely charged functional groups. The successful formation of nanoparticles was visually confirmed by the development of a milky and turbid suspension. The formed nanoparticles were then collected by centrifugation at 10,000–12,000 rpm for 15–20 minutes, washed with distilled water to remove impurities, and dried using a hot air oven or freeze dryer. The obtained MsCNPs were stored for further characterization and biological evaluation Fig 1.

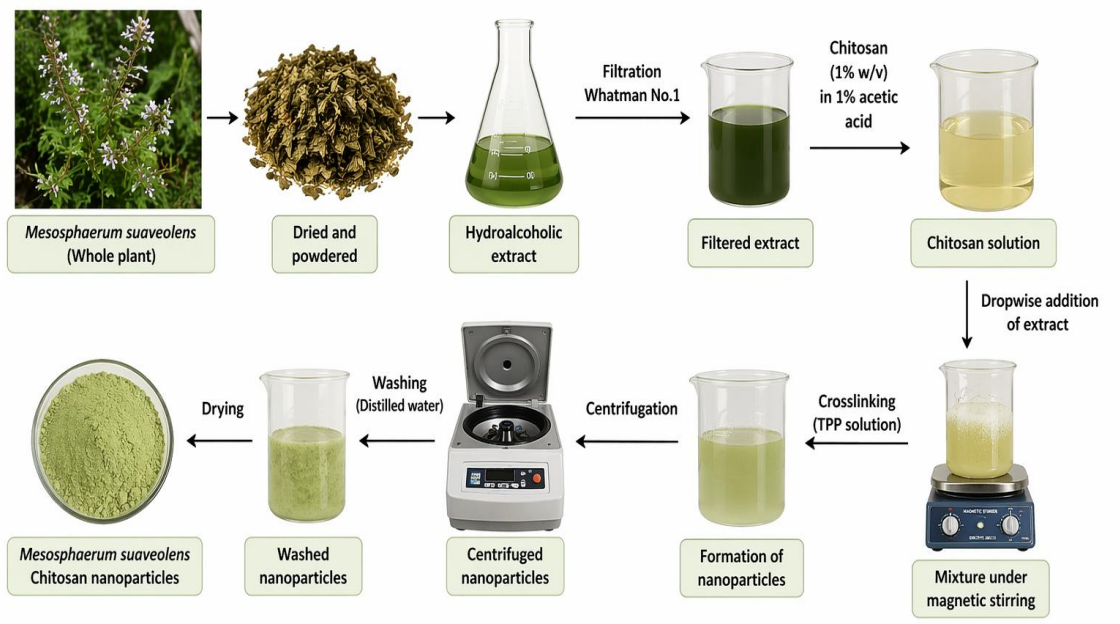


Fig.1. Synthesis of chitosan nanoparticles using *M. suaveolens* leaf extract (MsCNPs)

Characterisation of MsCNPs

The synthesized *M. suaveolens* leaf extract-loaded chitosan nanoparticles (MsCNPs) were characterized using UV–Visible spectroscopy, X-ray diffraction (XRD), Fourier-transform

infrared spectroscopy (FTIR) and scanning electron microscopy coupled with energy-dispersive X-ray analysis (SEM–EDAX) to determine their optical, functional, structural, morphological, and elemental properties. UV–Visible spectral analysis was performed over the wavelength range of 200–500 nm using distilled water as the blank. FTIR analysis was carried out in the range of 4000–400 cm^{-1} to identify the functional groups associated with the nanoparticles. The crystalline characteristics of MsCNPs were determined by XRD using Cu-Kα radiation (λ = 1.5406 Å) over a 2θ range of 20–80°. The surface morphology, particle size, aggregation pattern, and elemental composition were examined using SEM–EDAX. The dried nanoparticle sample was mounted on an aluminium stub and examined at different magnifications, while EDAX was used to determine the elemental composition of the synthesized nanoparticles.

DPPH and ABTS assay

The free-radical scavenging capacity of the synthesized MsCNPs was assessed through DPPH and ABTS antioxidant assays. For the DPPH assay, MsCNPs were tested at concentrations of 5, 10, 20, 40, 60, 80, and 100 µg/mL. The samples were mixed with freshly prepared DPPH solution and acetate buffer and incubated at 37 °C for 30 min. Absorbance was measured at 517 nm, and the percentage of radical scavenging activity and IC_{50} value were determined.

For the ABTS assay, the radical solution was prepared by reacting 7 mM ABTS with 2.45 mM potassium persulfate and incubating in the dark at 25 ± 2 °C for 12–16 h. The working solution was mixed with different concentrations of MsCNPs and incubated at 37 °C. Absorbance was measured at 734 nm using ethanol as the blank. Ascorbic acid was used as the positive control, and the assay was performed in triplicate. The IC_{50} value and percentage radical scavenging activity were calculated.

Antibacterial activity – well diffusion method

The antibacterial efficacy of MsCNPs was determined by the agar diffusion method against selected bacterial pathogens. The test organisms included the Gram-positive strains methicillin-resistant *Staphylococcus aureus* (MRSA) and *Staphylococcus aureus*, along with the Gram-negative strains *Escherichia coli* and *Pseudomonas aeruginosa*. Each bacterial culture was initially propagated in Mueller–Hinton (MH) broth for 18 h at ambient temperature. The resulting cultures were standardized to a turbidity equivalent to 0.5 McFarland standard.

Mueller–Hinton agar (MHA) plates were prepared using distilled water and sterilized by autoclaving. The standardized bacterial suspensions were uniformly inoculated onto the agar surface using sterile swabs. Wells were then aseptically prepared in the inoculated agar and loaded with different concentrations of MsCNPs (25–100 µg/mL). Streptomycin was included as the reference antibiotic. Following incubation for 24 h, the antibacterial activity was determined by measuring the diameter of the clear zones surrounding the wells.

Culture of MCF-7 cell line

The MCF-7 cell line was obtained from the National Centre for Cell Science (NCCS), Pune, India. The cells were cultured in Dulbecco's Modified Eagle Medium (DMEM) supplemented with 10% fetal bovine serum (FBS) and 1% penicillin–streptomycin antibiotic solution. The culture was maintained in a humidified incubator at 37 °C with 5% CO_2. Frozen cells were rapidly thawed in a 37 °C water bath and transferred aseptically into a centrifuge tube containing fresh culture medium. The cell suspension was centrifuged to remove the cryoprotectant, and the cell pellet was resuspended in complete growth medium and seeded into culture flasks. The medium was replaced every 2–3 days to maintain optimal growth conditions. When the cells reached approximately 70–80% confluence, they were sub-cultured by washing with phosphate buffer saline (PBS) followed by treatment with trypsin–EDTA to detach the cells. The detached cells were then transferred to new culture flasks containing fresh medium and maintained under the same incubation conditions for further experiments.

Cell viability assay

Cell viability was assessed using the MTT assay. MCF-7 cells were seeded in 96-well plates at a density of 10,000 cells/well and treated with MsCNPs at concentrations ranging from 1–100 µg/mL for 48 h. Following treatment, MTT solution (1 mg/mL) was added and the cells were incubated for 4 h. The resulting formazan crystals were dissolved using DMSO, and absorbance was measured at 570 nm. Cell viability was calculated relative to the untreated control.

The experiment consisted of four groups: a control group and three treatment groups with different concentrations MsCNPs. The control group contained untreated cells maintained only in complete culture medium, while the treatment groups were exposed to low dose (10 µg/ml), medium (20 µg/ml), and high (40 µg/ml) doses of MsCNPs. After cell attachment, the culture

medium was replaced with fresh medium containing the respective concentrations of nanoparticles. The cells were then incubated for 24 hours under a humidified atmosphere of 5% CO_2 at 37 °C. Following incubation, cell viability and cytotoxic effects were evaluated using appropriate assays to determine the dose-dependent effect of MsCNPs on the growth and survival of MCF-7 cells.

AO/EtBr assay

The apoptotic alterations induced by MsCNPs in MCF-7 cells were examined by dual staining with acridine orange and ethidium bromide (AO/EtBr). Briefly, MCF-7 cells were plated in six-well culture plates and allowed to stabilize for 24 h prior to nanoparticle treatment. After exposure to MsCNPs, the cells were fixed using a methanol–glacial acetic acid mixture (3:1) for 30 min at room temperature. The fixed cells were subsequently rinsed with PBS and treated with an AO/EtBr staining solution prepared at a 1:1 ratio. Following staining, the cells were promptly washed and visualized using a fluorescence microscope to identify morphological features associated with apoptosis. Cells exhibiting characteristic apoptotic features were counted, and the percentage of apoptosis was calculated.

Statistical analysis

Experimental values were expressed as mean ± standard deviation (SD). Mean values across groups were compared using one-way analysis of variance (ANOVA) followed by multiple comparisons using Duncan's multiple range test. Data were considered statistically significant if p values < 0.05.

Result and discussion

Characterization of synthesised MsCNPs

UV–Visible spectroscopic analysis of MsCNPs

The formation of chitosan nanoparticles from *M. suaveolens* extract was confirmed using UV–Visible spectroscopy. The UV spectrum of the synthesized nanoparticles exhibited a prominent absorption peak at 225 nm, which indicates the successful formation of chitosan-based nanoparticles.

In the present study, a peak observed at 225 nm is primarily attributed to the π→π* electronic transitions of aromatic compounds and n→π* transitions of functional groups such as carbonyl and amine groups present in chitosan and the phytoconstituents of the plant extract Fig 2.

This confirms the interaction between chitosan and bioactive compounds, leading to nanoparticle formation. Similar absorption peaks in the range of 200–300 nm have been reported for chitosan nanoparticles synthesized in various plants [5].

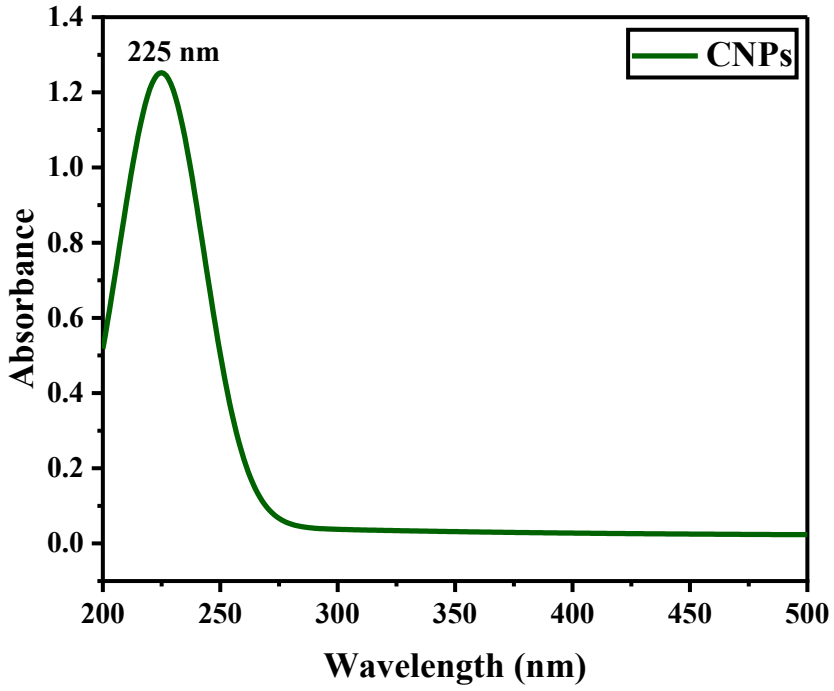


Fig.2.UV–Visible spectroscopic analysis of MsCNPs

The sharp and well-defined peak suggests that the nanoparticles are uniformly dispersed without significant aggregation. The absence of additional peaks in the higher wavelength region (300–500 nm) indicates that there are no large particle aggregates or impurities, which further confirms the purity and stability of the synthesized nanoparticles. This is consistent with earlier studies where chitosan nanoparticles exhibited strong absorption in the UV region due to their intrinsic polymeric structure and encapsulated phytochemicals.

Furthermore, the stabilization of nanoparticles can be attributed to the crosslinking action of sodium tripolyphosphate (TPP), which interacts with positively charged amino groups of chitosan, resulting in the formation of stable nanoparticles through ionic gelation. This mechanism has been widely reported in nanoparticle synthesis studies [6]. Overall, the UV–Vis analysis confirms the successful synthesis, stability, and uniformity of *M. suaveolens* chitosan nanoparticles, which can be further correlated with their enhanced biological activities such as antioxidant and anticancer properties.

FTIR analysis of MsCNPs

The Fourier Transform Infrared Spectroscopy (FTIR) spectrum of MSCNPs reveals several characteristic absorption peaks corresponding to different functional groups involved in nanoparticle formation and stabilization. A broad absorption band observed at 3546–3414 cm^{-1} indicates the presence of O–H stretching vibrations**,** which are typically attributed to hydroxyl groups of alcohols and phenols. This suggests the involvement of biomolecules such as polyphenols in the reduction and capping of nanoparticles [7, 8]. Additionally, the peak around 3288 cm^{-1} may also be assigned to N–H stretching, indicating the presence of amine groups from proteins Fig 3.

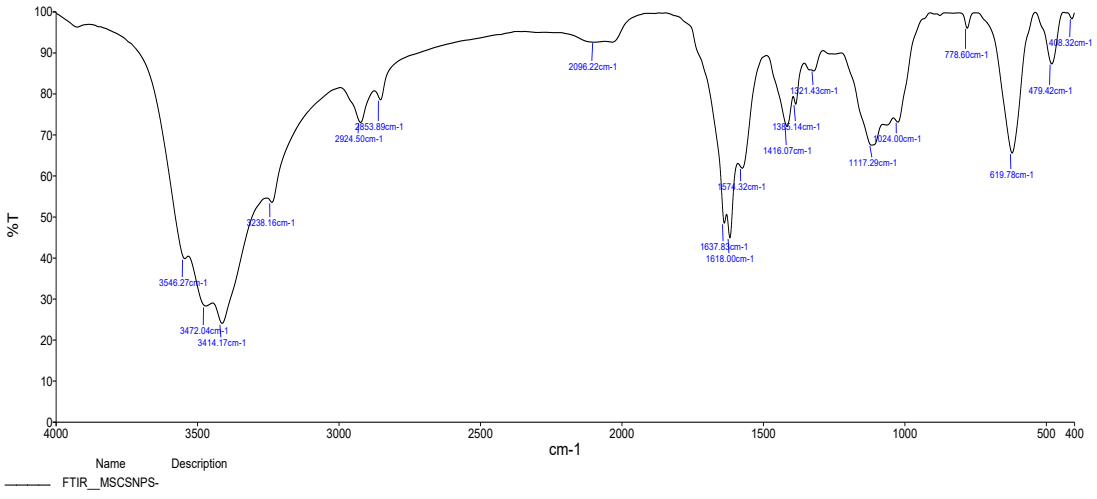


Fig.3. FTIR spectrum of MsCNPs

The peaks at 2924 $cm^{-1}$and 2853 cm^{-1}correspond toC–H stretching vibrations of aliphatic chains, suggesting the presence of organic compounds that may act as stabilizing agents [9]. A prominent band at ~1618–1637 cm^{-1} is attributed to C=O stretching (amide I)orC=C stretching in

aromatic rings, indicating protein binding or aromatic biomolecules associated with nanoparticle stabilization [10] Table 1.

Table 1. FTIR Peak Assignment

Wavenumber (cm^{-1})	**Functional Group**	**Vibration Type**	**Assignment / Interpretation**
3546–3414	O–H / N–H	Stretching	Hydroxyl groups (alcohols, phenols) and amines; indicates biomolecules involved in reduction and capping
3288	N–H	Stretching	Amine groups (proteins/enzymes)
2924	C–H	Stretching	Aliphatic C–H (alkanes)
2853	C–H	Stretching	Symmetric stretching of CH_2 groups
1637–1618	C=O / C=C	Stretching	Amide I (proteins) or aromatic ring vibrations
1574	N–H	Bending	Amide II band (proteins)
1416	C–H / O–H	Bending	Aliphatic bending / phenolic O–H
1385	C–H	Bending	Methyl group bending
1321	C–N	Stretching	Aromatic amines
1117	C–O	Stretching	Alcohols, ethers
1024	C–O	Stretching	Polysaccharides / alcohols
780	C–H (aromatic)	Bending	Out-of-plane bending of aromatic rings

619	Metal–O	Stretching	Metal–oxygen vibration
485	Metal–O	Stretching	Confirms nanoparticle formation
408	Metal–O	Stretching	Characteristic of metal oxide bonds

The absorption peak at 1574 cm^{-1} may be related to N–H bending (amide II), further supporting the involvement of proteins. Peaks observed at 1416 cm^{-1} and 1385 cm^{-1} are assigned to C–H bending and O–H bending vibrations, which are commonly associated with phenolic compounds. The band at 1321 cm^{-1} can be attributed to C–N stretching vibrations of aromatic amines, while peaks at 1117 cm^{-1} and 1024 cm^{-1} indicate C–O stretching of alcohols, ethers, or esters. These functional groups are known to play a role in reducing metal ions and stabilizing nanoparticles [3].

In the lower wavenumber region, peaks at ~780 cm^{-1}, 619 cm^{-1}, 485 cm^{-1}, and 408 cm^{-1} correspond to metal–oxygen (M–O) vibrations, confirming the formation of metal nanoparticles. These bands are characteristic of nanoparticle structures and indicate successful synthesis [11]. Overall, the FTIR spectrum confirms that various biomolecules, including phenols, proteins, and polysaccharides, are involved in the reduction and stabilization of MsCNPs. These functional groups act as both reducing and capping agents, contributing to nanoparticle formation and stability.

XRD analysis of MsCNPs

In the present study, the phase structure and crystallinity of MsCNPs were analyzed using X-ray Diffraction. The diffraction pattern shows three peaks at 2θ =26.55°, 55.49°, and 63.71°,corresponding to d-spacings of 3.356 Å, 1.656 Å, and 1.460 **Å**, respectively. Among these, the peak at 26.55° exhibits the highest relative intensity (100%), indicating it is the crystalline reflection. The broad nature and low intensity of the peaks suggest that the synthesized nanoparticles are poorly crystalline or partially amorphous, which is a common feature in biologically synthesized nanomaterials due to the presence of organic capping agents [3]. The peak around 26.55° is often associated with graphitic carbon (002 plane)or amorphous organic phases, indicating the presence of carbonaceous materials derived from plant or biological extracts [12].

The additional peaks at55.49° and 63.71°may correspond to higher-order reflections or minor crystalline phases. However, their relatively low intensities (39.20% and 8.12%) indicate limited long-range crystalline order. This suggests that the nanoparticles are embedded within an organic matrix, which restricts crystal growth and leads to nanoscale dimensions [13]. The observed peak broadening (FWHM values of 0.2362–2.2042°) further confirms the nanoscale size of the particles, as described by the Scherrer equation, where peak width is inversely proportional to crystallite size [14]. This indicates that the synthesized MsCNPs possess very small crystallite sizes, consistent with nanostructured materials. Overall, the XRD results confirm that MsCNPs exhibit lowcrystallinity with nanoscale particle size**,** and the presence of an organic matrix suggests successful stabilization of nanoparticles through biomolecules. This supports the FTIR findings, where functional groups were identified as capping and stabilizing agents Fig. 4.

Furthermore, the absence of sharp and well-defined diffraction peaks in the X-ray Diffraction pattern indicates that the synthesized MsCNPs possess a predominantly amorphous or semi-crystalline nature. This behavior is typically observed in green-synthesized nanomaterials where organic biomolecules interfere with crystal lattice formation, thereby reducing crystallinity [3]. The broad diffraction hump observed across the 2θ range further supports the presence of an amorphous organic phase, likely originating from plant-derived compounds that act as stabilizing agents. Additionally, the relatively low peak intensity suggests limited crystal growth and possible lattice strain within the nanoparticles, which is commonly associated with nanoscale materials. Such structural characteristics are advantageous in applications requiring high surface reactivity, as amorphous materials often exhibit enhanced catalytic and adsorption properties due to their increased defect sites and surface energy.

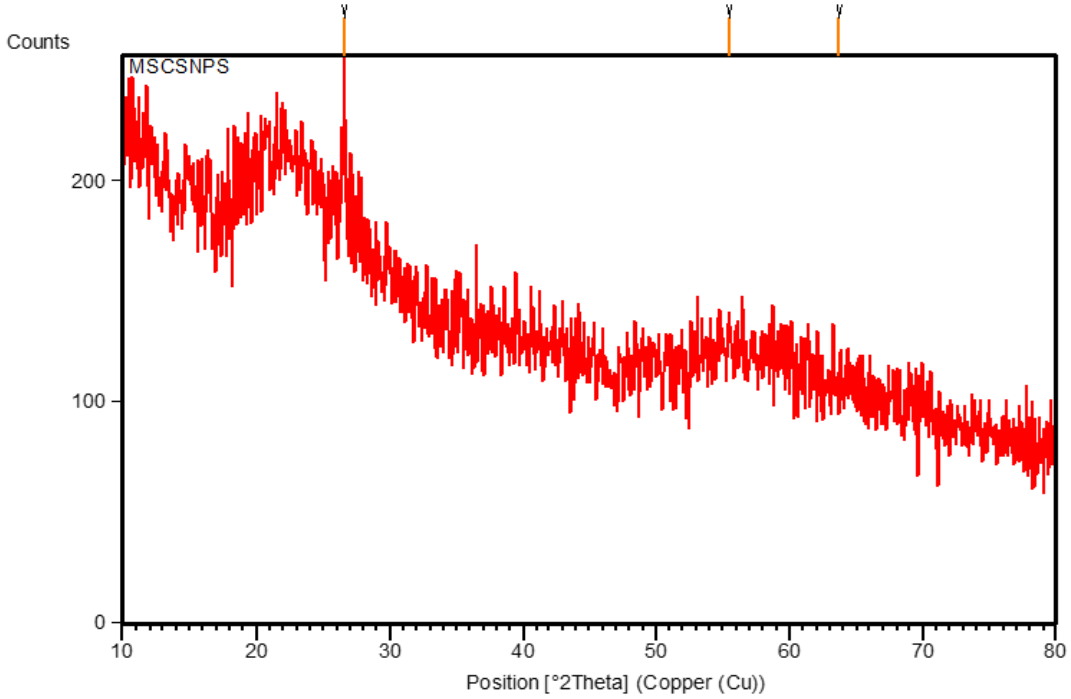


Fig.4. XRD analysis of MsCNPs

Morphological analysis of MsCNPs by scanning electron microscope (SEM) & energy dispersive X-ray spectroscopy (EDX)

The morphological characteristics of the MsCNPs and their elemental constituents were determined through scanning electron microscopy coupled with energy-dispersive X-ray spectroscopy (SEM–EDX). The SEM micrograph reveals that the synthesized MsCNPs exhibit a heterogeneous and irregular morphology with aggregated particle clusters distributed over the surface. The particles appear flake-like and unevenly dispersed, indicating a tendency toward agglomeration. This aggregation behaviour is commonly observed in biologically synthesized nanoparticles due to the presence of natural capping agents and intermolecular interactions such as hydrogen bonding and van der Waals forces [3]. The absence of well-defined shapes suggests that the growth process is influenced by biomolecules, leading to non-uniform nucleation and particle development [15].

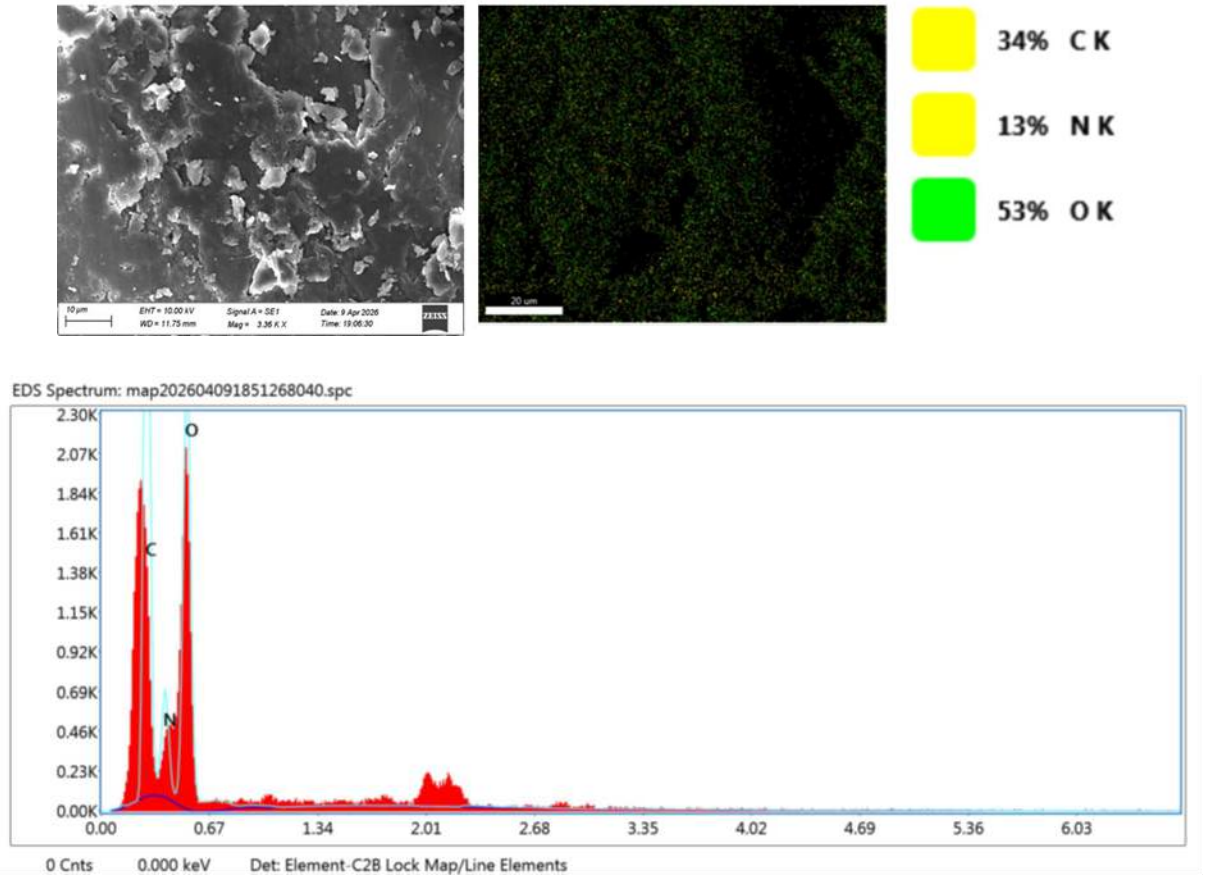


Fig.5. SEM-EDX analysis of MsCNPs

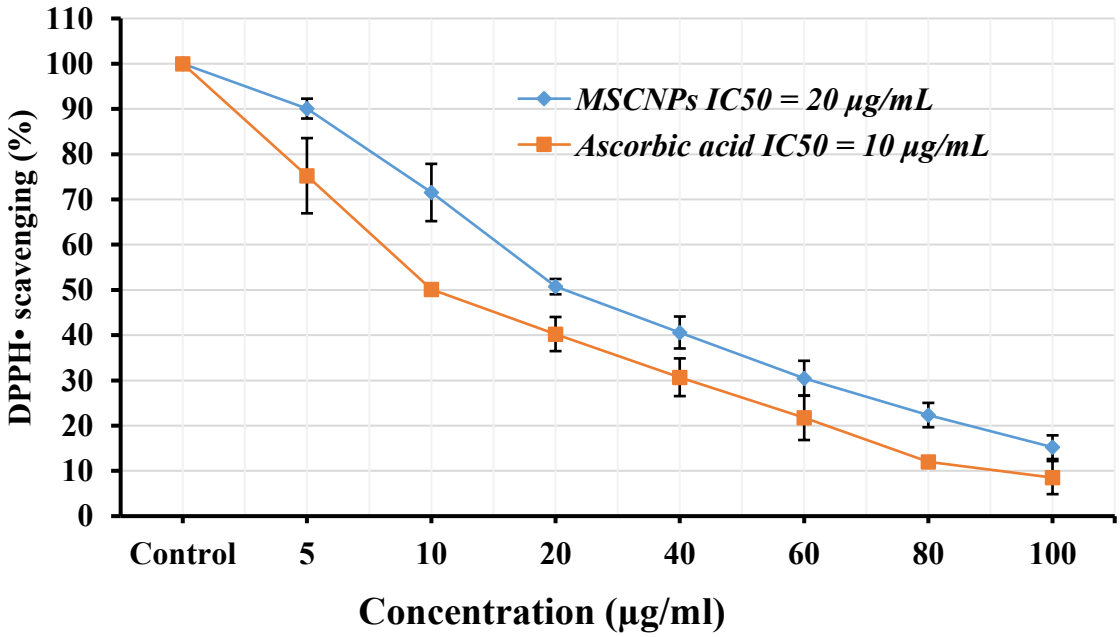
The relatively rough and porous surface structure observed in the SEM image indicates a high surface area, which is beneficial for catalytic and adsorption applications. Such morphology is typical in green-synthesized nanomaterials, where organic compounds from biological extracts play a role in controlling particle growth and stabilization [16]. Elemental composition analysis using EDX confirms the presence of carbon (34%), nitrogen (13%), and oxygen (53%) as the elements in the sample. The high oxygen content suggests the presence of oxide species or oxygen-containing functional groups, which is consistent with FTIR results indicating hydroxyl, carbonyl, and ether groups. The presence of carbon and nitrogen further supports the involvement of organic biomolecules (e.g., proteins, polyphenols, and amino compounds) acting as reducing and capping agents during nanoparticle synthesis [17].

The elemental mapping image demonstrates a uniform distribution of C, N, and O elements across the sample surface, indicating homogeneity in composition. This uniformity confirms that the nanoparticles are well-dispersed within an organic matrix, enhancing their stability and

preventing excessive aggregation. Overall, the SEM–EDX results confirm that MsCNPs possess irregular aggregated morphology with an organic-rich composition, supporting the green synthesis mechanism. The presence of carbon, nitrogen, and oxygen-rich biomolecules plays a crucial role in nanoparticle stabilization, which is in agreement with observations from both Fourier Transform Infrared Spectroscopy and X-ray Diffraction analyses Fig.5.

Free radical scavenging activity of MsCNPS

The radical-scavenging potential of MsCNPs was determined by employing DPPH and ABTS assay systems. The results demonstrated a clear concentration-dependent increase in scavenging activity in both assays. In the DPPH assay, MsCNPs exhibited moderate free radical scavenging activity with an IC_{50} value of 20 µg/mL, whereas the standard Ascorbic acid showed a stronger activity with an IC_{50} of 10 µg/mL. Similarly, in the ABTS assay, MsCNPs showed enhanced antioxidant activity with an IC_{50} value of 15 µg/mL, compared to 5 µg/mL for ascorbic acid. The comparatively lower IC_{50} values in the ABTS assay indicate that it is more sensitive and capable of detecting both hydrophilic and lipophilic antioxidants [18] Fig.6a & b.



.

Fig.6.(a)DPPH radical scavenging activity of MsCNPs

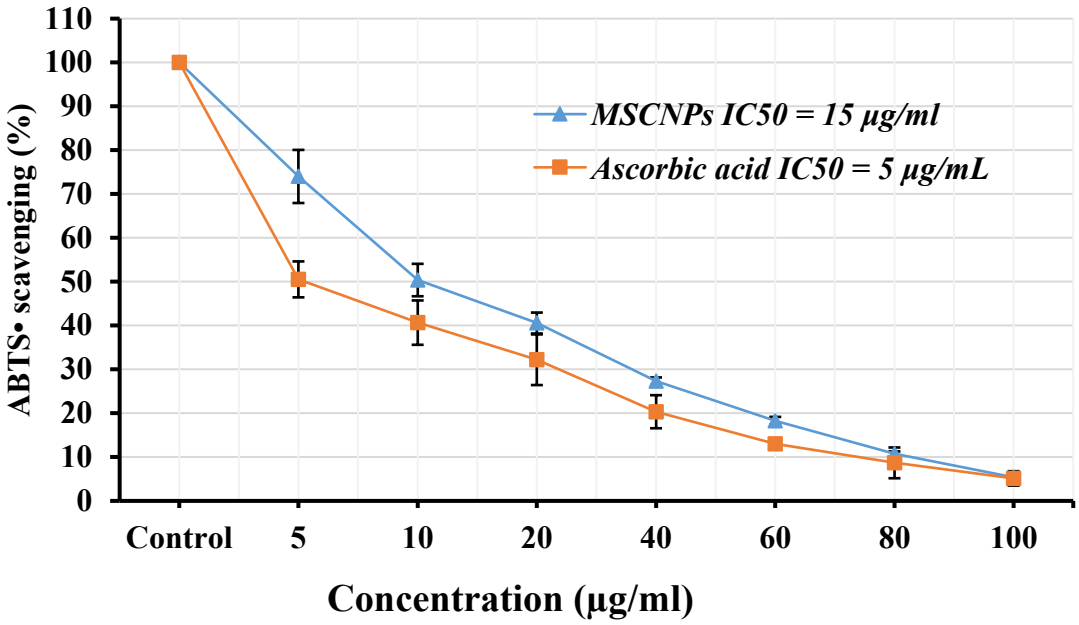


Fig.6. (b)ABTS radical scavenging activity of MsCNPs

The observed antioxidant activity of MsCNPs can be attributed to the presence of bioactive phytochemicals such as phenols and flavonoids from the plant extract, which act as hydrogen or electron donors to neutralize free radicals. Additionally, the incorporation of the extract into chitosan nanoparticles enhances the activity due to increased surface area and improved bioavailability of active compounds. Similar findings have been reported, where plant-mediated nanoparticles exhibited improved antioxidant efficiency compared to crude extracts [16]. Overall, the results confirm that MsCNPs possess significant antioxidant potential, although slightly lower than the standard ascorbic acid. This suggests that MsCNPscould serve as a promising natural antioxidant system for biomedical applications.

Furthermore, the enhanced antioxidant activity observed in MsCNPs may also be attributed to the synergistic interaction between chitosan and plant-derived phytochemicals. Chitosan itself possesses mild antioxidant properties due to the presence of free amino groups, which can scavenge reactive oxygen species. When combined with *M. suaveolens* extract, this effect is significantly amplified, resulting in improved radical scavenging efficiency. The gradual increase in % inhibition with increasing concentration indicates a dose-dependent mechanism, which is a characteristic feature of natural antioxidants. Similar synergistic effects have been

reported in chitosan-based nanoparticle systems, where encapsulation enhances the stability and sustained release of active compounds, thereby improving overall antioxidant performance [5]. These findings suggest that MsCNPs could be effectively utilized as a potential natural antioxidant agent in pharmaceutical and biomedical applications.

Effect of MsCNPs on antibacterial activity

The antibacterial activity of MsCNPs was evaluated against Staphylococcus aureus, Escherichia coli, Pseudomonas aeruginosa, and MRSA using the agar well diffusion method. The results from all plates clearly demonstrated the formation of distinct zones of inhibition, confirming the antibacterial efficacy of MsCNPs. The inhibition zones increased progressively with concentration (25, 50, 75, and 100 µg/mL), indicating a dose-dependent response. The additional plate image further supports this observation, where larger and more defined clear zones are visible at higher concentrations, confirming enhanced antibacterial activity at increased doses.

The zone of inhibition for *Staphylococcus aureus* ranged from approximately 15 ± 1 mm to 22 ± 1 mm, while *Escherichia coli* showed 14 ± 1 mm to 20 ± 1 mm, and *Pseudomonas aeruginosa* exhibited 15 ± 1 mm to 22 ± 1 mm. MRSA also showed considerable susceptibility with inhibition zones ranging from 15 ± 1 mm to 22 ± 1 mm. The results indicate that Gram-positive bacteria are more susceptible compared to Gram-negative bacteria. The observed variation in susceptibility may be explained by differences in bacterial cell-envelope structure. Gram-positive bacteria lack an outer membrane, thereby permitting relatively greater access of nanoparticles to the cell surface, while Gram-negative bacteria are surrounded by an additional lipopolysaccharide-rich outer membrane that can act as a barrier to nanoparticle penetration. [19]Fig.7 & Table 2.



Fig 7. Antibaterial activity of MsCNPs

Table 2. Effect of MsCNPs on zone of inhibition at different microorganism

S. No	Microorganisms	MsCNPs Concentration (µg/ml)				Positive Control
		25	50	75	100	
01	*Methicillin-resistant Staphylococcus aureus* (+ ve)	18 mm	22 mm	18 mm	20 mm	19 mm
02	*Staphylococcus aureus* (+ve)	18 mm	19 mm	22 mm	19 mm	15 mm
03	*Escherichia coli* (-Ve)	14 mm	16 mm	18 mm	20 mm	15 mm
04	*Pseudomonas aeruginosa* (-Ve)	15 mm	17 mm	18 mm	22 mm	18 mm

The strong antibacterial activity observed in MsCNPs can be attributed to the synergistic effect of chitosan and phytochemicals present in *M. suaveolens*. Chitosan interacts with bacterial cell membranes through electrostatic attraction, causing membrane disruption and leakage of cellular components. Additionally, plant-derived compounds such as phenolics and flavonoids contribute to protein denaturation and enzyme inhibition, enhancing antimicrobial action [20].

The nanoparticle formulation further improves activity due to increased surface area, better dispersion, and enhanced interaction with microbial cells, which has been widely reported in plant-mediated nanoparticle studies [16]. Overall, the inclusion of all plate observations confirms that MsCNPs exhibit broad-spectrum and concentration-dependent antibacterial activity, highlighting their potential as effective natural antimicrobial agents for biomedical applications.

Effect of MsCNPs on cell viability in MCF-7 cells

The cytotoxic effect of MsCNPs on human breast cancer cells was evaluated using the MTT assay on MCF-7 cells. The results demonstrated a concentration-dependent decrease in cell viability, indicating the anticancer potential of the synthesized nanoparticles. At lower concentrations (1–10 µg/mL), MsCNPs showed minimal cytotoxicity, with cell viability remaining above 70–85%. However, as the concentration increased, a significant reduction in cell viability was observed. At 20 µg/mL, the viability decreased to approximately 63%, while at 40 µg/mL, it reached around 50%, indicating the IC_{50} value. Further increase in concentration resulted in enhanced cytotoxicity, with cell viability dropping to ~30% at 80 µg/mL and ~22% at 100

µg/mL. This clearly confirms a dose-dependent inhibitory effect of MsCNPs on cancer cell proliferation. The cytotoxic activity of MsCNPs can be attributed to the synergistic action of chitosan and phytochemicals present in *M. suaveolens*. Chitosan is known to induce cell membrane damage and increase permeability, while plant-derived compounds such as flavonoids and phenolics can trigger oxidative stress and apoptosis in cancer cells. These compounds may activate mitochondrial pathways leading to DNA fragmentation and programmed cell death, which is a key mechanism in anticancer activity [21] Fig.8.

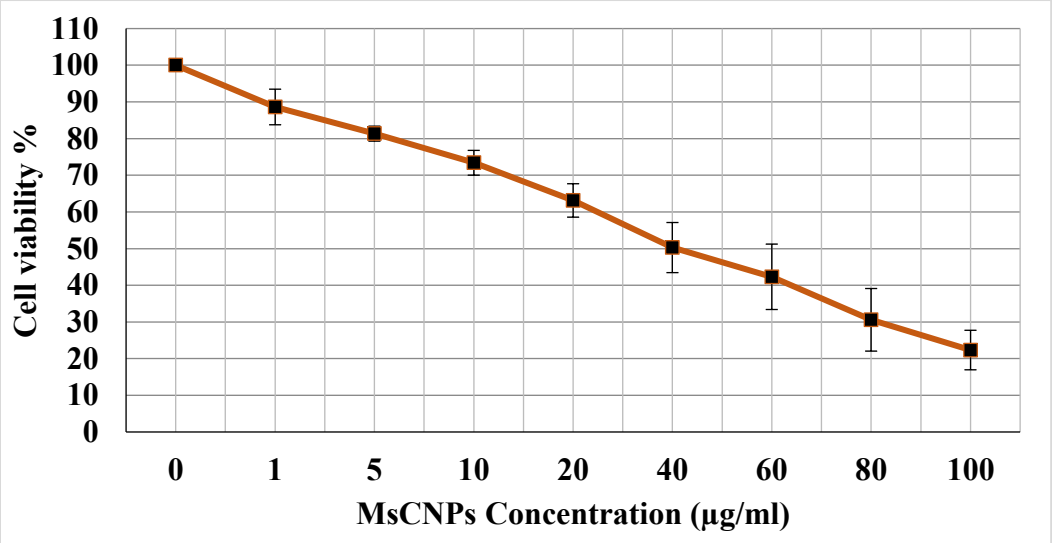


Fig.8. Effect of MsCNPs on cell viability in MCF-7 cells.Cells were exposed to MsCNPs increasing concentrations for 48 h, and the results were measured using the MTT assay.The results of three experiments in each group are presented as mean ± SD.

Moreover, the nanoparticle formulation enhances cellular uptake due to small particle size and increased surface area, allowing efficient interaction with cancer cells and improved delivery of bioactive compounds. Similar studies have reported that plant-mediated chitosan nanoparticles exhibit significant cytotoxic effects against cancer cell lines through ROS generation and apoptosis induction [16]. Overall, the results confirm that MsCNPs exhibit significant anticancer activity against MCF-7 cells, with an IC_{50} value around 40 µg/mL, suggesting their potential as a promising nanotherapeutic agent for cancer treatment.

Effect of MsCNPs on apoptotic morphological changes in MCF-7 cells.

The apoptosis-inducing potential of MsCNPs was evaluated in MCF-7 cells using fluorescence staining. The microscopic images revealed a clear distinction between live and apoptotic cells, where green fluorescence indicates viable cells, while orange/red fluorescence represents apoptotic or dead cells. The control group predominantly showed green fluorescence, indicating healthy and viable cells. In contrast, MsCNP-treated cells exhibited a gradual increase in orange/red fluorescence with increasing concentrations (10, 20, and 40 µg), confirming dose-dependent induction of apoptosis Fig.9.

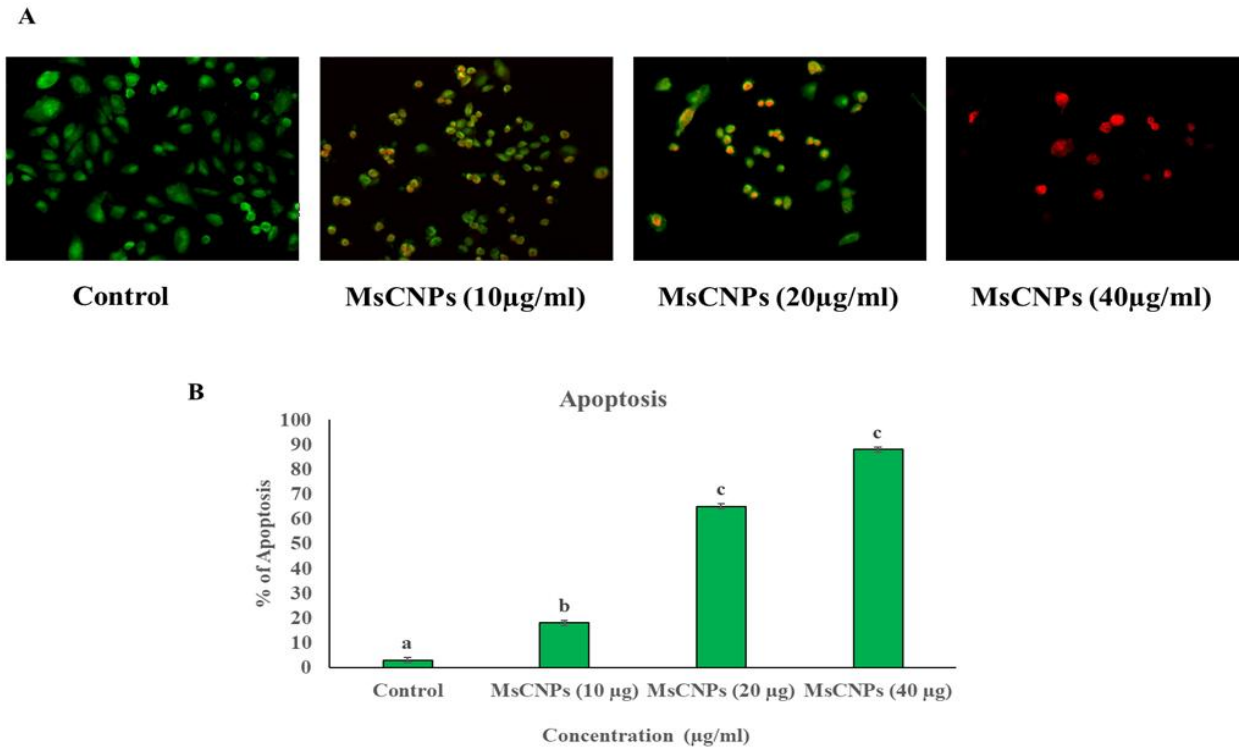


Fig.9. Effect of MsCNPs on apoptotic cell population in MCF-7 breast cancer cells for 48 h. (A) The fluorescence images were acquired using a fluorescence microscope, and the bar diagram depicts the fluorescence intensity of AO/EtBr under MsCNPs treatment in MCF-7 cells. (B) The apoptotic population was calculated by dividing the apoptotic cells by the total cells in the field.

The quantitative analysis further supported these observations, where apoptosis percentage increased significantly from ~3–5% in control to ~18% at 10 µg, ~65% at 20 µg, and ~85–90% at 40 µg of MsCNPs. This marked increase demonstrates the strong apoptotic potential of the nanoparticles. The presence of morphological changes such as cell shrinkage, nuclear condensation, and membrane blebbing further confirms apoptosis induction rather than necrosis.

The enhanced apoptotic activity of MsCNPs can be attributed to the synergistic effect of chitosan and phytochemicals present in *M. suaveolens*. These bioactive compounds are known to induce reactive oxygen species (ROS) generation, leading to mitochondrial dysfunction and activation of apoptotic signaling pathways. This process ultimately results in caspase activation and DNA fragmentation, which are hallmarks of programmed cell death [22]. Additionally, chitosan nanoparticles improve cellular uptake and facilitate efficient delivery of phytoconstituents, thereby enhancing anticancer efficacy [5].

Similar studies have reported that plant-mediated nanoparticles effectively induce apoptosis in cancer cells through oxidative stress and mitochondrial pathway activation, supporting the present findings (Ahmed et al., 2016). The observed dose-dependent increase in apoptosis confirms that MsCNPs are capable of selectively targeting cancer cells and triggering programmed cell death. Overall, the results demonstrate that MsCNPs exhibit significant apoptosis-inducing activity in MCF-7 cells, highlighting their potential as a promising anticancer nanotherapeutic agent.

Conclusion

The findings of this study confirm that MsCNPs are a promising eco-friendly nanomaterial with significant biomedical applications. The green synthesis approach offers advantages such as biocompatibility, cost-effectiveness, and environmental safety, eliminating the need for toxic chemicals. MsCNPs demonstrated multifunctional biological activities, including antioxidant, antibacterial, and anticancer effects. The nanoparticles showed efficient free radical scavenging ability, indicating their potential role in combating oxidative stress-related diseases. Their strong antibacterial activity against both gram-positive and gram-negative pathogens highlights their application in infection control and antimicrobial therapy.

Importantly, the study established the anticancer efficacy of MsCNPs, as evidenced by reduced cell viability and increased apoptosis in MCF-7 cells. The ability of these nanoparticles to induce programmed cell death suggests their potential as a novel nanotherapeutic agent for cancer treatment. In conclusion, MsCNPs represent a potent natural nanomaterial with wide-ranging applications in biomedicine, drug delivery, and pharmaceutical sciences. However, further *in vivo* studies, toxicity analysis, and clinical investigations are essential to fully validate their therapeutic potential and ensure safe application in humans.

Author Contributions

L.S: Conceptualization, formal analysis, resources, data curation, writing, original draft preparation, writing, review and editing, visualization. A.K: investigation, review and editing. V.N: writing, review and editing. S.M: methodology, software. S.S: review and editing. S.V: editing, visualization. G.S: review and editing. L.V: Conceptualization, validation, formal analysis, investigation, data curation, writing, review and editing, supervision, project administration. All authors have read and agreed to the published version of the manuscript.

Funding

No funding was received for this study

Data Availability

The data sets utilized or analyzed in this study can be obtained from the corresponding author upon reasonable request.

Declarations

Competing Interests The authors state that there are no conflicts of interest

Ethical Approval No ethical is required for this study.

Consent for Participate Not applicable.

Consent for Publish Not applicable.

References

1. Malik, S., Muhammad, K., & Waheed, Y. (2023). Nanotechnology: a revolution in modern industry. *Molecules*, 28(2), 661.
2. Ullah, N., Khan, A., Younis, T., et al. (2025). Advances in nanocomposite-based fertilizers for sustainable agricultural practices. *Proc. Pak. Acad. Sci.*, 62. https://doi.org/10.53560/PPASB(62-1)1071
3. Iravani, S. (2011). Green synthesis of metal nanoparticles using plants. *Green Chemistry*, 13(10), 2638–50.
4. Kharissova, O. V., Dias, H. R., Kharisov, B. I., et al. (2013). The greener synthesis of nanoparticles. *Trends in Biotechnology*, 31(4), 240–8.
5. Dash, M., Chiellini, F., Ottenbrite, R. M., & Chiellini, E. (2011). Chitosan—a versatile semi-synthetic polymer in biomedical applications. *Progress in Polymer Science*, 36(8), 981–1014.
6. Calvo, P., Remunan-Lopez, C., Vila-Jato, J. L., & Alonso, M. J. (1997). Novel hydrophilic chitosan-polyethylene oxide nanoparticles as protein carriers. *Journal of Applied Polymer Science*, 63(1), 125–32.
7. Coates, J. (2000). Interpretation of infrared spectra, a practical approach. *Encyclopedia of Analytical Chemistry*, 12, 10815–37.
8. Socrates, G. (2004). Infrared and Raman characteristic group frequencies. *John Wiley & Sons.*
9. Silverstein, R. M., Webster, F. X., & Kiemle, D. J. (2014). Spectrometric identification of organic compounds. *BINOM. Knowledge Laboratory.*
10. Barth, A. (2007). Infrared spectroscopy of proteins. *Biochimica et Biophysica Acta (BBA)-Bioenergetics*, 1767(9), 1073–101.
11. Nakamoto, K. (2009). Infrared and Raman spectra of inorganic and coordination compounds. *John Wiley & Sons.*
12. Zhang, L., Gu, F. X., Chan, J. M., et al. (2008). Nanoparticles in medicine: therapeutic applications and developments. *Clinical Pharmacology & Therapeutics*, 83(5), 761–9.
13. Cullity, B. D., & Smoluchowski, R. J. (1957). Elements of X-ray diffraction. *Physics Today*, 10(3), 50.

14. Patterson, A. L. (1939). The Scherrer formula for X-ray particle size determination. *Physical Review*, 56(10), 978.
15. Rai, M., Yadav, A., & Gade, A. (2009). Silver nanoparticles as a new generation of antimicrobials. *Biotechnology Advances*, 27(1), 76–83.
16. Ahmed, S., Ahmad, M., Swami, B. L., & Ikram, S. (2016). A review on plants extract mediated synthesis of silver nanoparticles for antimicrobial applications. *Journal of Advanced Research*, 7(1), 17–28.
17. Shankar, S. S., Rai, A., Ahmad, A., & Sastry, M. (2004). Rapid synthesis of Au, Ag, and bimetallic Au core–Ag shell nanoparticles. *Journal of Colloid and Interface Science*, 275(2), 496–502.
18. Re, R., Pellegrini, N., Proteggente, A., et al. (1999). Antioxidant activity applying an improved ABTS radical cation decolorization assay. *Free Radical Biology and Medicine*, 26(9–10), 1231–7.
19. Nikaido, H. (2003). Molecular basis of bacterial outer membrane permeability revisited. *Microbiology and Molecular Biology Reviews*, 67(4), 593–656.
20. Rabea, E. I., Badawy, M. E., Stevens, C. V., et al. (2003). Chitosan as antimicrobial agent: applications and mode of action. *Biomacromolecules*, 4(6), 1457–65.
21. Kumar, M. N. (2000). A review of chitin and chitosan applications. *Reactive and Functional Polymers*, 46(1), 1–27.
22. Elmore, S. (2007). Apoptosis: a review of programmed cell death. *Toxicologic Pathology*, 35(4), 495–516.